

A Mechanism of Primary Photoactivation Reactions of Rhodopsin: Modeling of the Intermediates in the Rhodopsin Photocycle

Masaji Ishiguro

Contribution from the Suntory Institute for Bioorganic Research, 1-1 Wakayamadai, Shimamoto, Osaka 618-8503, Japan

Received June 22, 1999. Revised Manuscript Received November 15, 1999

Abstract: The photoisomerization of the retinylidene chromophore and the process of thermal relaxation of its strained conformation were examined by restrained molecular dynamic simulations in the transmembrane model of rhodopsin. This model was constructed based on the projection map obtained by electron cryomicroscopy. The photoconversion process from the 11-*cis*-retinylidene chromophore to the all-trans chromophore was traced by simultaneous rotation of the adjacent C12–C13 bond, leading to an all-trans chromophore having a C11–C12-twisted and C12–C13-*s-cis* conformation for the bathorhodopsin chromophore. In accord with the characteristic CD signals at 500 and 540 nm, the retinylidene chromophore of rhodopsin and bathorhodopsin showed characteristic right-handed and left-handed helical conformations, respectively. Subsequent rotation of the C12–C13 bond led to the lumirhodopsin chromophore with an all-trans C12–C13-*s-trans* conformation, affecting the backbone structure of transmembrane helix 3 by steric interaction between the 13-Me group of the chromophore and opsin. The conformational change of the chromophore from lumirhodopsin to metarhodopsin I placed the β -ionyl portion of the chromophore in an alternate binding site and the protonated Schiff base in a position appropriate for proton transfer to its counterion, Glu113. Estimation of UV absorption of the rhodopsin and photoactivated rhodopsin chromophores indicated the importance of the PSB–Glu113 carboxylate distance, the twist of the C11–C12 double bond, and the C12–C13 *s-cis* conformation of the 11,13-diene portion to the bathochromic shift of bathorhodopsin.

Introduction

The visual pigment rhodopsin is a seven-helix integral membrane protein, opsin (Figure 1), with an 11-*cis*-retinylidene chromophore (Figure 2) bound to Lys296 of the protein via a protonated Schiff base (PSB). Light causes an extremely rapid 11-*cis* to all-trans isomerization of the chromophore.¹ The following bleaching intermediates are observed along the photoactivation cascade. The initial photoproduct, photorhodopsin,² rapidly decays to the first stable photointermediate, bathorhodopsin (Batho). Batho already contains a photoisomerized all-trans retinal chromophore and slowly decays with conformational changes to metarhodopsin I (Meta I) via lumirhodopsin (Lumi). Upon deprotonation of the Schiff base in Meta I, a slower conformational change yields metarhodopsin II (Meta II), which activates the G protein transducin. Subsequent conversion to metarhodopsin III (Meta III) releases the all-trans retinal by Schiff base hydrolysis and generates opsin.^{3,4} It has been demonstrated that Batho is also generated from 9-*cis*-retinal-bound rhodopsin (isorhodopsin).⁵ These photochemical isomerizations and the subsequent thermal conformational changes of the chromophore are exquisitely controlled by opsin. Thus, elucidation of the opsin-bound chromophore conformations and chromophore–opsin interactions should provide a further understanding of the photochemical event.

Rhodopsin and the photointermediates are characterized by UV absorption of the chromophore. The retinylidene chro-

mophore bound to opsin shows a longer absorption maximum ($\lambda_{\max} = 498$ nm) than a nonprotein bound protonated Schiff base of 11-*cis*-retinal (440 nm). Batho shows a further bathochromic shift at 540 nm. Blue shifts are observed during conversion from Batho to Lumi (497 nm) and from Lumi to Meta I (478 nm). Semiempirical quantum chemical calculation suggested plausible structural origins for the red shifts, such as twist of the double bonds,⁶ charge separation between the PSB and its counterion,⁷ and distribution of negative charge along the conjugated chain of the chromophore.⁸

Three-dimensional structure of bovine rhodopsin has been solved by electron cryomicroscopy at low resolution.⁹ The structure shows a characteristic arrangement of the seven-helix bundle, which has a three-layered structure and is closely packed toward the intracellular side. On the other hand, a high-resolution three-dimensional structure of bacteriorhodopsin has been solved by electron cryomicroscopy^{10,11} and X-ray crystallography.^{12,13} The structure precisely showed the location of all-trans retinal

(6) Korenstein, R.; Muszkat, K. A.; Sharafy-Ozeri, S. *J. Am. Chem. Soc.* **1973**, *95*, 6177.

(7) Blatz, P. E.; Mohler, J. H.; Navangul, H. V. *Biochemistry* **1972**, *11*, 848.

(8) Honig, B.; Greenberg, A. D.; Dinur, U.; Ebrey, T. G. *Biochemistry* **1976**, *15*, 4593.

(9) Unger, V. M.; Hargrave, P. A.; Baldwin, J. M.; Schertler, G. F. X. *Nature* **1997**, *389*, 203.

(10) Henderson, R.; Baldwin, J. M.; Ceska, T.; Zemlin, F.; Beckman, F.; Downing, K. *J. Mol. Biol.* **1990**, *213*, 899.

(11) Kimura, Y.; Vassilyev, D. G.; Miyazawa, A.; Kidera, A.; Matsushima, M.; Mitsuoka, K.; Murata, K.; Hirai, T.; Fujiyoshi, Y. *Nature* **1997**, *389*, 206.

(12) Pebay-Peyroula, E.; Rummel, G.; Rosenbush, J. P.; Landau, E. M. *Science* **1997**, *277*, 1676.

(13) Luecke, H.; Richter, H.-T.; Lanyi, J. K. *Science* **1998**, *280*, 1934.

(1) Khorana, H. G. *J. Biol. Chem.* **1992**, *267*, 1.

(2) Shichida, Y.; Matsuoka, S.; Yoshizawa, T. *Photobiochem. Photobiophys.* **1984**, *7*, 221.

(3) Rando, R. R. *Chem. Biol.* **1996**, *3*, 255.

(4) Sakmar, T. P. *Prog. Nucleic Acid Res.* **1998**, *59*, 1.

(5) Yoshizawa, T.; Wald, G. *Nature* **1963**, *197*, 1279.

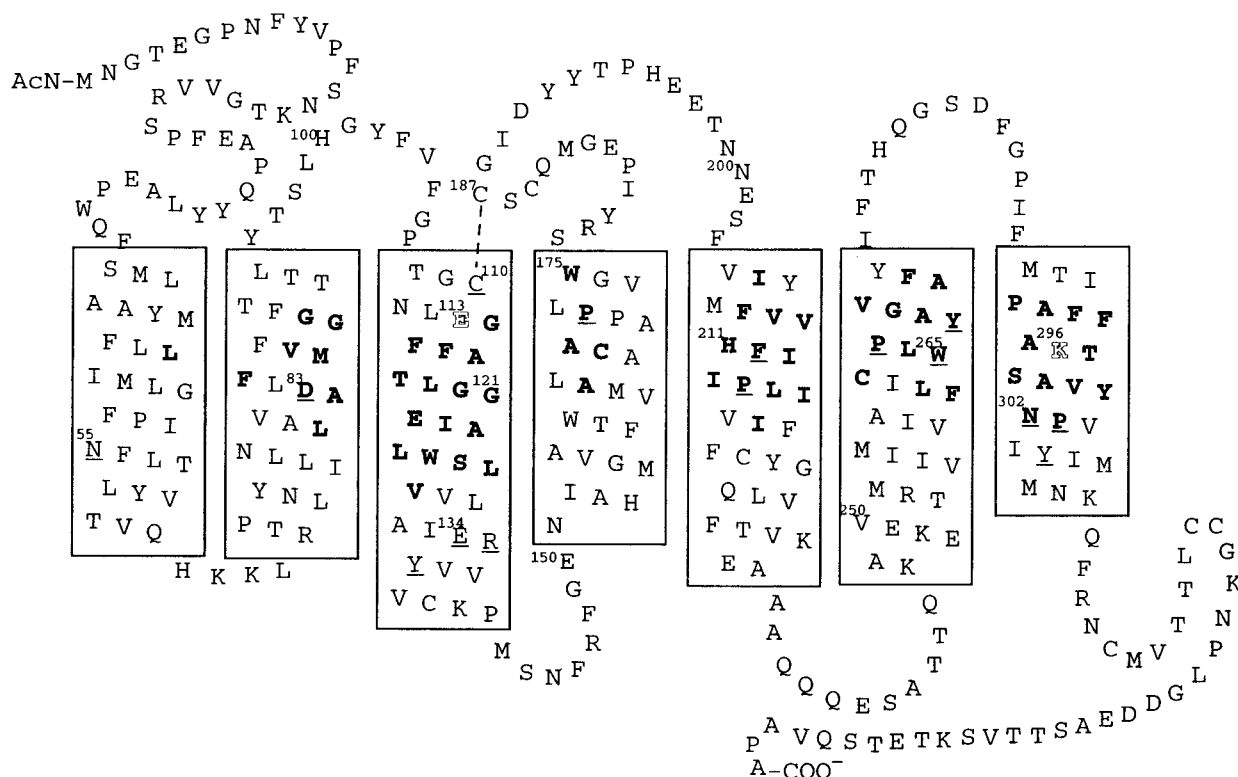


Figure 1. Schematic representation of bovine rhodopsin secondary structure based on the model built by Baldwin et al. The amino terminus and extracellular surface are toward the top and the carboxyl terminus and intracellular surface are toward the bottom of the figure. Structurally important C110 and C187 are connected by a broken line. Residues within 8 Å distance from the chromophore are indicated by bold letters. E113 and K296, specific residues in mammalian rhodopsin, are shown by outlined letters. Underlined letters indicate highly conserved residues among G protein-coupled receptors.

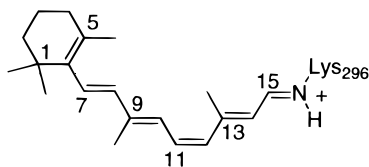


Figure 2. Labeling convention for the 11-*cis*-retinylidene Schiff base.

connected to Lys216 via a Schiff base. However, comparison of the transmembrane helices of rhodopsin with those of bacteriorhodopsin revealed remarkable structural differences in their helix lengths and arrangement.⁹ The 11-*cis*-retinylidene chromophore **1** in rhodopsin forms the PSB with Lys296 in an anti mode^{14,15} and the 9-methyl group is suggested to be proximal to Gly121 and/or Phe261.¹⁶ The C6–C7 bond forms an *s-cis* conformation,¹⁴ whereas the other single bonds, C8–C9, C10–C11, C12–C13, and C14–C15, have *s-trans* conformations.¹⁵ Solid-state NMR measurement of the ¹³C-labeled 11-*cis*-retinylidene chromophore indicated that the C10–C11 bond is twisted.¹⁷

Results of the photoisomerization experiment using 10-fluoro- and 12-fluoro-analogues of 9-*cis*- and 11-*cis*-retinals implied that the isomerization of the C9–C10 or C11–C12 double bond accompanies rotation of the C13–C15 portion and the Lys296

residue, but keeps the β -ionone moiety in place.¹⁸ The circular dichroism (CD) spectrum of Batho shows a negative sign opposite to that of rhodopsin, indicating that the Batho chromophore has a conformation distinct from that of rhodopsin at the C9–C13 portion.¹⁹ Resonance Raman spectra of Batho also suggest an all-*trans* chromophore twisted at the C11–C12 double bond and also at the C10–C11 and C12–C13 single bonds.²⁰ Difference FTIR spectra between Batho and rhodopsin suggest that the opsin structure is kept unchanged during the photoisomerization of the retinylidene chromophore while water molecules at the binding cleft change their hydrogen-bonding modes.²¹

The strong negative CD signal of Batho changes to a weak negative signal in Lumi, suggesting a further conformational change of the C9–C13 portion,¹⁹ even though Lumi is photochemically convertible to rhodopsin. Once Meta I is reached, its structure is irreversible to the preceding intermediates. The relation between the conformational change of the chromophore and the change of the CD spectra has not been well understood, and lack of 3D-structural information on rhodopsin precludes a model that can account for the CD spectra.

Meta II, a photoactivated and functionally active form of rhodopsin, appears to have an arrangement of the transmembrane helices distinct from that of rhodopsin. Recent paramagnetic resonance spectra on spin-labeled rhodopsin mutants in inactive and active forms indicated rigid-body motions of the trans-

(14) Smith, S. O.; Palings, I.; Copie, V.; Raleigh, D. P.; Courtin, J.; Pardoen, J. A.; Lugtenburg, J.; Mathies, R. A.; Griffin, R. G. *Biochemistry* **1987**, *26*, 1606.

(15) Palings, I.; Pardoen, J. A.; van den Berg, E.; Winkel, C.; Lugtenburg, J.; Mathies, R. A. *Biochemistry* **1987**, *26*, 2544.

(16) Han, M.; Groesbeek, M.; Sakmar, T. P.; Smith, S. O. *Proc. Natl. Acad. Sci. U.S.A.* **1997**, *94*, 13442.

(17) Feng, X.; Verdegem, P. J. E.; Lee, Y. K.; Sandstrom, D. J.; Eden, M.; Bovee-Geurts, P.; de Grip, W. J.; Lugtenburg, J.; de Groot, H. J. M.; Levitt, M. H. *J. Am. Chem. Soc.* **1997**, *119*, 6853.

(18) Shichida, Y.; Ono, T.; Yoshizawa, T.; Matsumoto, H.; Asato, A. E.; Zingoni, J. P.; Liu, R. S. H. *Biochemistry* **1987**, *26*, 4422.

(19) Horiuchi, S.; Tokunaga, F.; Yoshizawa, T. *Biochim. Biophys. Acta* **1980**, *591*, 445.

(20) Eyring, G.; Curry, B.; Broek, A.; Lugtenburg, J.; Mathies, R. *Biochemistry* **1982**, *21*, 384.

(21) Kandori, H.; Maeda, A. *Biochemistry* **1995**, *34*, 14220.

membrane helices in the photoactivation process.^{22,23} Models for the photoisomerization of the chromophore have been proposed, but without consideration of structural restraints imposed by the opsin structure due to lack of structural information on the protein. The bicycle-pedal model proposed by Warshell requires rotation of two double bonds (11-cis bond and the Schiff base double bond).²⁴ Another model, so-called the concerted twist model proposed by Liu and Asato, involves the rotation of the C10–C11 or C12–C13 single bond together with the 11-cis double bond.^{25,26}

Three-dimensional models of the transmembrane 7- α -bundle of rhodopsin have been constructed based on the projection map obtained by the electron cryomicroscope.^{27,28} However, no chromophore structure of the photoactivated rhodopsins such as Batho, Lumi, and Meta I has been elucidated as a complex structure with opsin.

This report describes the model building study of the photoactivated rhodopsins using restrained molecular dynamics. The starting structure was based on the C α structural model of opsin constructed by Baldwin et al.,²⁹ which is so far the most reliable structure of the transmembrane helices. The structures of the photoactivated retinylidene chromophores were generated in the binding cleft. The photoactivated rhodopsin models suggest structures of the retinylidene chromophore in the primary photoconversion and plausible interactions between the chromophore and opsin in the photoactivation process. The structures of the chromophore in the photocascade also account for the signs of CD spectra of rhodopsin and Batho as well as the shifts of the UV absorption maxima of Batho, Lumi, and Meta I.

Experimental Section

Opsin. Herein the three-dimensional C α -structure model of the transmembrane helices of opsin constructed by Baldwin et al.²⁹ was used for the modeling study of rhodopsin. The backbone amide and side-chain structures were generated by use of a biopolymer module installed in Insight II (ver. 97.2, Molecular Simulations Inc., San Diego, CA). Severe steric interactions of side chains were removed using a rotamer database installed in Insight II. Molecular dynamics calculation on the backbone amide and side-chain structures was performed at 400 K with 8 Å cutoff, a dielectric constant of 1, and a time step of 1 fs for 100 ps by sampling a conformation every 1 ps by use of Discover 3 (ver. 97.2, Molecular Simulations Inc.). Structure minimization was carried out until the final root-mean-square deviation (rmsd) became less than 0.1 kcal mol⁻¹/Å. The most energetically favored transmembrane structure of opsin was selected from the generated 100 structures. The conditions described above were applied to molecular dynamics/minimization procedures unless otherwise mentioned.

Rhodopsin. A retinal derived from the crystal structure of 11-*cis*-retinal^{30,31} was manually docked into the cleft of opsin, forming the protonated Schiff base at N ζ of Lys296. Molecular dynamics/minimiza-

tion at 298 K was carried out with a distance restraint of 3.6 Å using a force constant of 10 kcal mol⁻¹/Å² for the C9 methyl carbon to C ζ of Phe261 and with restraints of trans configuration (180° as the targeted value) for the C7–C8, C9–C10, C13–C14, and C15–N ζ double bonds, cis configuration (0°) for the C11–C12 double bond, and a twist (+40°) for the C6–C7 bond, while shell residues, which consist of residues farther than 8 Å from the chromophore, were fixed. The shell residues are indicated in bald face type in Figure 1. A torsional strength of 50 kcal/mol was used for restraining dihedral angles unless otherwise mentioned. The functional forms used for distance and torsion restraints are shown in eqs 1 and 2, respectively:

$$E = K(R_{ij} - R_{\text{target}})^2 \quad (1)$$

where K is a force constant, R_{ij} is the current distance between the atoms, and R_{target} is the target distance;

$$E = V[1 + \cos(n\phi - \phi_0)] \quad (2)$$

where V is the strength of the restraint, n (1 was used in this study) is an integer periodicity, and ϕ_0 is the phase angle.

Water molecules were disposed of manually by checking short contacts with the structurally optimized rhodopsin model. Then, the water structure was optimized by use of Discover 3.

Bathorhodopsin. Restrained molecular dynamics was performed at 298 K for 20 ps on the rhodopsin structure while restraining the C9–C10 and C13–C14 double bonds in a trans configuration and enforcing a trans configuration on the C11–C12 double bond with a torsional strength of 50 kcal/mol. The β -ionone portion (C1–C9) of the chromophore and all atoms of opsin were frozen except for the side-chain portion of Lys296. Then, the mobile portion of each conformation was optimized in the frozen cleft without restraint for the double bonds.

Lumirhodopsin. Restrained molecular dynamics was performed on the Batho structure at 298 K while restraining the acyclic double bonds (C7–C8, C9–C10, C11–C12, C13–C14, and C15–N ζ) into a trans configuration as well as enforcing the C12–C13 bond into an *s*-trans (180°) conformation with a torsional strength of 50 kcal/mol. Each conformation was minimized without restraint on the C12–C13 bond. The shell residues which consist of residues farther than 8 Å from the chromophore were fixed during the above procedure. The cyclohexenyl moiety was tethered at the original position using a force constant of the restraint of 5 in eq 3:

$$E = \sum K_i(R_i - R_i^{\text{original}})^2 \quad (3)$$

where K_i is a force constant, R_i is the current position, and R_i^{original} is the original position.

Metarhodopsin I. While restraining the C5–C6–C7–C8 torsion angle at 40° and the acyclic double bonds at 180°, molecular dynamics and the subsequent structure minimization were carried out on the Lumi structure for 300 ps at 298 K, sampling a conformation every 3 ps, and only freezing the shell portion which consists of residues farther than 8 Å from the chromophore.

UV Absorption Maxima and Heats of Formation of the Intermediates. The acetic acid portion of the Glu113 residue and the methylamine portion of the Lys296 residue as well as the entire chromophore were separated from the opsin structure. The heats of formation of the rhodopsin and Batho chromophore structures were estimated by use of the semiempirical quantum chemical method PM3. Two Batho rotamers 1 and 2 were generated by rotation of the C11–C12 bond of the Batho chromophore. UV absorption maxima for the model intermediates were then derived from the S₀ → S₁ transition energies using the ZINDO program installed in insightII.

Results

Rhodopsin Structure Model. A recent study using the retinal analogues modified at the C9 methyl group and the Gly121 mutants of opsin has suggested interactions between the C9 methyl group of the retinylidene chromophore and Gly121 on transmembrane helix 3 (TM3). Cooperatively between Gly121

(22) Resek, J. F.; Farahbakhsh, Z. T.; Hubell, W. L.; Khorana, H. G. *Biochemistry* **1993**, *32*, 12025.

(23) Farrens, D. L.; Altenbach, C.; Yang, K.; Hubbell, W. L.; Khorana, H. G. *Science* **1996**, *274*, 768.

(24) Warshell, A. *Nature* **1976**, *260*, 679.

(25) Liu, R. S. H.; Asato, A. E. *Proc. Natl. Acad. Sci. U.S.A.* **1985**, *82*, 259.

(26) Asato, E. A.; Denny, M.; Liu, R. S. H. *J. Am. Chem. Soc.* **1986**, *108*, 5052.

(27) Herzyk, P.; Hubbard, R. E. *Biophys. J.* **1995**, *69*, 2419.

(28) Pogocheva, I. D.; Lomize, A. L.; Mosberg, H. I. *Biophys. J.* **1997**, *70*, 1963.

(29) Baldwin, J. M.; Schertler, G. F. X.; Unger, V. M. *J. Mol. Biol.* **1997**, *272*, 144.

(30) Gilardi, R. D.; Karle, I. L.; Karle, J. *Acta Crystallogr.* **1972**, *B28*, 2605.

(31) Drikos, G.; Ruppel, H.; Dietrich, H.; Sperling, W. *FEBS Lett.* **1982**, *131*, 23.

and Phe261 on TM6 in binding the chromophore was also suggested,¹⁶ even though the long distance between C α of Gly121 and that of Phe261 (11.3 Å) should hardly realize a direct interaction between these residues.²⁹ Thus, shape complementarity may exist among the two residues and the chromophore. Careful observation of the model shows that the proS hydrogen of Gly121 points in a direction opposite to Phe261. This implied that not only the C9 methyl group but also another group in the chromophore is required to accomplish the steric complementarity.

Shifting our attention to the PSB proton, this should be oriented away from the Glu113 carboxylate (oriented toward the intracellular site) *before* the photoisomerization since the PSB portion flips over during the photoisomerization cascade¹⁸ and transfers its proton to Glu113 at the Meta II stage. Taking into account that the chromophore is approximately parallel to the membrane plane, as estimated from polarized light spectra,³² a suitable binding site for the C9 methyl group was limited to the area near the aromatic residue of Phe261. At this location, the C9 methyl group was oriented toward the proR hydrogen of Gly121, whereas the proS hydrogen of Gly121 was lying close to the C13 methyl group. This finding completes the missing piece in the steric complementarity among Gly121, Phe261, and the chromophore. It suggests that steric interactions of the C9 and C13 methyl groups with Phe261 and Gly121, respectively, link the two spatially separated residues.

Restrained molecular dynamics on the rhodopsin structure, allowing motion of the backbone atoms in the vicinity of the chromophore, brought about average dihedral angles of 167° (164–169°) and 171° (168–173°) for C9–C10–C11–C12 and C11–C12–C13–C14, respectively, which accompanied minor deformation around Ala117 on TM3 (rmsd value of 0.38 for the backbone atoms) and Ala295 on TM7 (rmsd value of 0.44 for the backbone atoms). The dihedral angle for C9–C10–C11–C12 in the most stable conformation was smaller than the value (~160°) estimated from solid-state NMR measurements.¹⁷ For C12–C13, the ~10° bond twist was smaller than that observed in the crystal structure of 11-*cis*-retinal (38.3°)^{30,31} and that estimated from solid-state NMR measurements.³³ The narrow binding cleft for the C13 methyl group appears to bring about the smaller twists in the C11–C14 portion. It is tempting to assume that the highly conserved Pro303 residue causes a kink of TM7 allowing more space for a bent conformation at the C11–C14 portion. However, this model has no evident kink at Pro303. The plane containing the C7–C8 and C9–C10 double bonds of the chromophore formed a negative angle with the plane containing the C13–C14 and C15–N ζ double bonds. This dihedral angle is consistent with the first negative Cotton effect at 295 nm in the exciton-coupled CD measurement of the C11–C12 dihydroretinal analog-bound rhodopsin.³⁴

The model showed a characteristic binding mode of the chromophore (Figure 3). The 1,1-dimethyl group of the cyclohexenyl moiety lay on the Leu125 residue on TM4. Phe211 on TM5 made van der Waals contact with C2 and C4 of the cyclohexenyl moiety. Trp265 on TM6 formed a boundary for one face of the β -ionyl moiety (C3 and C5 through C9) at 3.5–4.0 Å. A photoaffinity-labeling experiment using a 3-diazo-4-keto retinal analogue has shown that the cyclohexenyl moiety resides proximal to Trp265.³⁵ Thr118, Gly121, and Glu122 on TM3 formed another wall opposite to the Trp265 residue. The

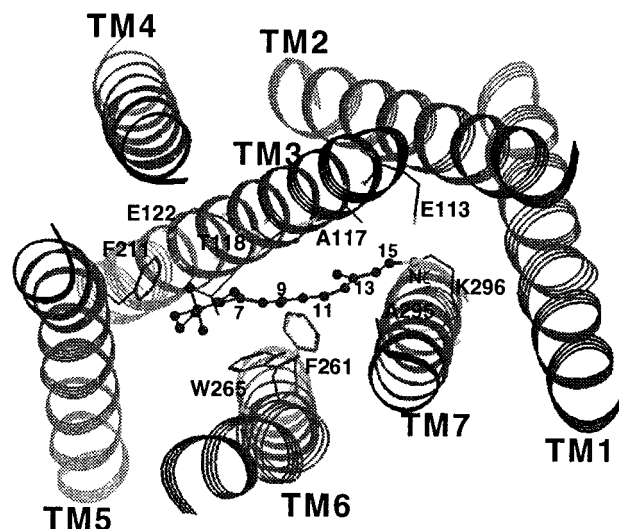


Figure 3. A view of the rhodopsin structure model from the extracellular site. Transmembrane helices (TM1–7) are depicted by a ribbon model. Retinylidene chromophore is shown by ball-and-stick notation and amino acid residues (one letter codes) important for chromophore binding are shown by stick notation. Black: Retinylidene chromophore and heteroatoms of residues other than the PSB nitrogen. Gray: Carbon atoms of residues.

protonated Glu122 carboxylic acid³⁶ resided 3.7 Å away from C6 of the chromophore and 3.3 Å away from the indole nitrogen of Trp126. The C13-methyl group was surrounded by the carbonyl oxygen of Ala117 and C α of Thr118 on TM3 and C β of Ala295 on TM7 at distances of 3.2, 4.2, and 3.7 Å, respectively. The α -carbon of Gly121 lay between the C9-methyl and C13-methyl groups at distances of 4.0 and 4.4 Å, respectively. In the Gly121Leu mutant, the Leu121 side chain occupies the space where the C13 methyl group is expected to exist. This causes alteration of the chromophore position compared to the wild-type complex and gives rise to a collision between the C9-methyl group and the Phe261 residue. The introduction of the ethylene group between C10 and the C13-methyl group facilitates the Gly121Leu mutant to activate transducin in the dark.³⁷ The model suggests the steric interactions between the ethylene group and the Leu121 residue. The C11 and C12 carbons were proximal to C α of Gly121 (3.5 Å) and the backbone amide oxygen of Ala295 (3.3 Å), respectively. The backbone oxygen of Ala295 was also close to C14 (3.2 Å). The C15 carbon was located between the Ala117 and Ala295 residues (4.0 and 3.8 Å, respectively). Thus, the chromophore was tightly held in the cleft.

The carboxylate oxygen atom (O ϵ_1) of Glu113 on TM3, the counterion of the PSB,³⁸ was located 5.4 Å away from the PSB nitrogen. The other oxygen atom (O ϵ_2) was located further away from the PSB nitrogen (5.8 Å). Although a close contact of the carboxylate with C12 has been assumed based on solid-state NMR measurement and empirical quantum chemical calculation,³⁹ the carboxylate of Glu113 was located far from C12 (9.0 Å). The present model had no appreciable space to accommodate another negative charge such as a carboxylate or a chloride ion near C12 except for the backbone carbonyl oxygen (3.3 Å).

(35) Zhang, H.; Lerro, K. A.; Yamamoto, T.; Lien, T. H.; Sastry, L.; Gawinowicz, M. A.; Nakanishi, K. *J. Am. Chem. Soc.* **1994**, *116*, 10165.

(36) Fahmy, K.; Jager, F.; Beck, M.; Zvyaga, T. A.; Sakmar, T. P.; Siebert, F. *Proc. Natl. Acad. Sci. U.S.A.* **1993**, *90*, 10206.

(37) Han, M.; Lou, J.; Nakanishi, K.; Sakmar, T. P.; Smith, S. O. *J. Biol. Chem.* **1997**, *272*, 23081.

(38) Sakmar, T. P.; Franke, R. R.; Khorana, H. G. *Proc. Natl. Acad. Sci. U.S.A.* **1989**, *86*, 8309.

(39) Han, M.; Smith, S. O. *Biochemistry* **1995**, *34*, 1425.

(32) Liebman, P. A. *Biophys. J.* **1962**, *2*, 161.

(33) Verdegem, P. J.; Bovee-Geurts, P. H.; de Grip, W. J.; Lugtenburg, J.; de Groot, H. J. *Biochemistry* **1999**, *38*, 11316.

(34) Tan, Q.; Lou, J.; Borhan, B.; Karnaukhova, E.; Berova, N.; Nakanishi, K. *Angew. Chem., Int. Ed. Engl.* **1997**, *36*, 2089.

Putative Water Molecule Structure around the Protonated Schiff Base. Water molecules near the PSB have been suggested from kinetic analysis of deuterium exchange experiments and FTIR measurements on the native and mutant rhodopsins.^{40,41} Space for a water molecule (W_1) was found at a site close to the PSB and the carboxylate. This water molecule could reside within hydrogen bond distance to the carboxylate oxygen ($O\epsilon_1$) within van der Waals contact with C15, $C\epsilon$ of Lys296 and the PSB nitrogen. The presence of a water molecule hydrogen bonded to Glu113 has been evidenced by FTIR measurements.⁴²

The presence of water molecules near the Asp83 residue and the Gly121 backbone carbonyl also has been suggested by difference FTIR measurements.⁴³ A cavity lined by small residues such as Ala82 on TM2, Gly120, Gly121, and Ala124 on TM3 and Ala299 on TM7 was found in the interior of the cleft. The hydrophilic surface of the cavity consisted of two highly conserved residues, Asp83 and Asn302 on TM 7 as well as the PSB nitrogen, suggesting the existence of water molecules in this location. The hydroxyl oxygen ($O\delta_1$) of the carboxylic acid of Asp83 could be a hydrogen bond acceptor since Asp83 shows a characteristically high $C=O$ stretching frequency (1767 cm^{-1}) for a carboxylic acid.^{36,44} Asn302 and the backbone amide carbonyl of Gly120 could also hydrogen bond to water molecules. Although the exact number, location, and orientation of water molecules is by no means definitive, at least three water molecules could be positioned interconnecting the hydrophilic moieties. The first water molecule (W_2) could be a hydrogen bond acceptor for the PSB proton and a hydrogen bond donor for Asp83. The second one (W_3) could be positioned between the backbone carbonyl oxygen of Gly120 and $O\delta_1$ of Asp83. The third one (W_4) could be located within hydrogen bond distance to the Asn302 residue.

The space lined by Ile48 on TM1, Met86, Val87, Gly90 on TM2, and Lys296 could be filled by three water molecules (W_5 – W_7) which interconnect the two distant water molecules (W_1 and W_2). With two or three water molecules (W_1 , W_5 , and W_6) the side chain of the Gly90Asp mutant could be accommodated.⁴⁵ Figure 4 depicts a putative hydrogen bond network among the water molecules and the hydrophilic moieties.

Photoactivated Retinal Chromophore. Twists of the single bonds, C12–C13 and C10–C11, have been suggested from calculations on the intensity of the hydrogen-out-of-plane (HOOP) modes of the Batho chromophore.⁴⁶ Resonance Raman spectra of Batho demonstrated that the C11–H and C12–H wags are virtually uncoupled,²⁰ suggesting a twisted C11–C12 double bond. Judging from the extraordinarily rapid ($<200\text{ fs}$) photoisomerization of the C11–C12 cis double bond, this reaction was assumed to affect a very limited part of the chromophore in the early bleaching intermediates leaving the rest of the retinylidene chromophore and the opsin structure unaffected. Hence, in the model building of the Batho structure, conformation of the C10–C15 portion of the chromophore and the Lys296 residue was examined in the rigid cleft of opsin. Restrained molecular dynamics and the subsequent structure minimization on the C10–C15 portion of the chromophore and

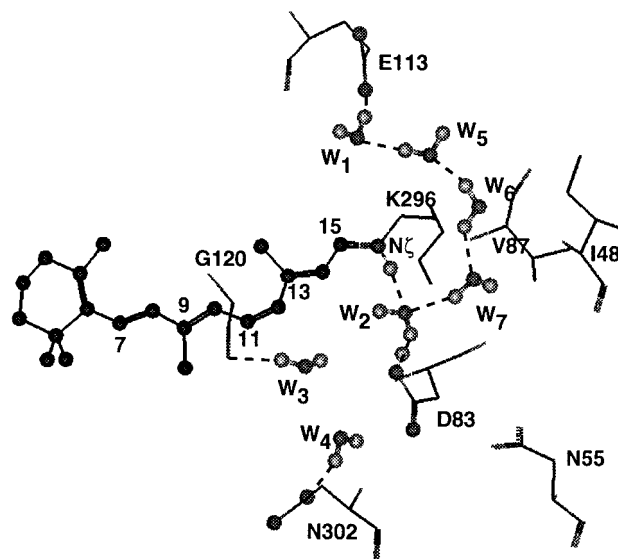


Figure 4. Water molecules (W_1 – W_7) around the PSB. Water molecules, the chromophore (black), and heteroatoms (deep gray) of side chains are shown by ball-and-stick notation. Broken lines indicate putative hydrogen bonds. Only hydrogens (light gray) for water molecules, carboxylic acid proton of Asp83, and the PSB are shown for clarity. Numberings for C7, C9, C11, C13, and C15 are given for the chromophore.

the side chain of Lys296 in the rigid opsin cleft while restraining the double bonds in the mobile portion into an all-trans configuration furnished the C11–C12 double bond-isomerized chromophore structures. All of the chromophore structures were essentially the same and had a twisted *s*-cis C12–C13 bond (-46° for C11–C12–C13–C14) and a twisted *s*-trans C10–C11 bond (-170° for C9–C10–C11–C12) together with a twisted C11–C12 double bond (-149° for C10–C11–C12–C13). The semiempirical quantum chemical calculation using PM3 suggested that the strained chromophore portion is 37.2 kcal/mol higher in energy than the rhodopsin chromophore. This value is in good agreement with the experimentally determined value ($\sim 35\text{ kcal/mol}$).⁴⁷

The C13 methyl group moved toward the Glu113 carboxylate (1.2 \AA) to adapt to the cis–trans isomerization. The movement of the PSB nitrogen resulted in a distance of 5.6 \AA between the PSB nitrogen and the carboxylate oxygen, which is slightly longer than that of rhodopsin. It then follows that the movement of the chromophore would influence the water molecules in its proximity. Figure 5 compares the chromophore structures of rhodopsin and Batho by superimposing the opsin structures.

The isomerized chromophore would thermally relax, gradually influencing the conformation of the opsin residues in the vicinity of the chromophore, and further conformational change of the chromophore restores a stable double bond from a strained and twisted double bond. In the decay of Batho to Lumi the β -ionyl moiety would be kept at a position similar to that of Batho, since Lumi is photoconvertible to rhodopsin.⁵ Thus, the mobile region for Lumi formation was extended to the C7–C15 portion of the chromophore and residues surrounding the chromophore. Conversion from the C12–C13 *s*-cis to the *s*-trans conformation accompanying simultaneous rotation of the Lys296 residue was expected to give rise to a Lumi conformation. However, even under forced conditions (a force constant of 100 kcal/mol for C11–C12–C13–C14), the conversion from *s*-cis to *s*-trans was not realized due to severe steric interactions between the 13-

(40) Deng, H.; Huang, L.; Callendar, R. H.; Ebrey, T. *Biophys. J.* **1994**, *66*, 1129.

(41) Maeda, A.; Ohkita, Y. J.; Sasaki, J.; Shichida, Y.; Yoshizawa, T. *Biochemistry* **1993**, *32*, 12033.

(42) Nagata, T.; Terakita, A.; Kandori, H.; Kojima, D.; Shichida, Y.; Maeda, A. *Biochemistry* **1997**, *36*, 6164.

(43) Nagata, T.; Terakita, A.; Kandori, H.; Shichida, Y.; Maeda, A. *Biochemistry* **1998**, *37*, 17216.

(44) West, R.; Korst, J. J.; Johnson, W. S. *J. Org. Chem.* **1960**, *25*, 1976.

(45) Rao, V. R.; Cohen, G. B.; Oprea, D. D. *Nature* **1994**, *367*, 639.

(46) Eyring, G.; Curry, B.; Mathies, R.; Fransen, R.; Palings, I.; Lugtenburg, J. *Biochemistry* **1980**, *19*, 2410.

(47) Cooper, A. *Nature* **1979**, *282*, 531.

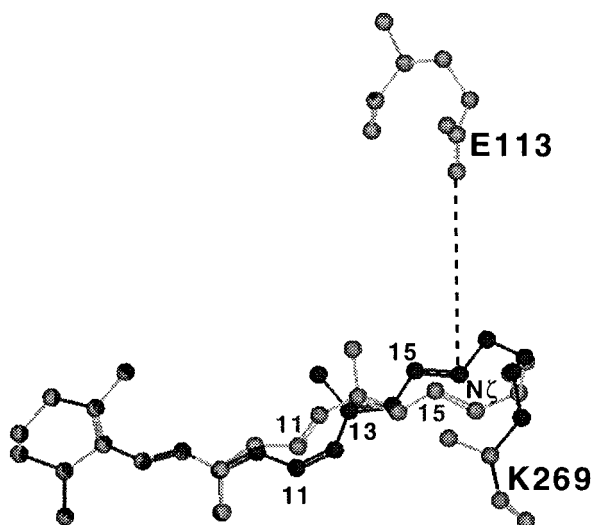


Figure 5. Lateral view of the chromophores of rhodopsin (black) and Batho (gray). Opsin structure except for Glu113 and Lys296 is omitted for clarity. E113, backbone of K296, and the C1–C8 portions of the chromophore of rhodopsin are overlapped with those of Batho.

methyl group and residues proximal to the methyl group, in particular, Ala117, Gly121, and Ala295 when all α -carbons were frozen. On the other hand, 13-demethylated retinylidene chromophore was readily converted to the C12–C13 *s*-trans structure using a force constant of 50 kcal/mol for C11–C12–C13–C14. This result implied that motion of the opsin structure is required to enable the rotation of the C12–C13 bond. Since Batho decays to Lumi in about 30 ns, the 13-methyl group would be able to induce partial deformation of TM3 and/or TM7 within this interval. Restrained molecular dynamics/minimization on the Batho chromophore at 298 K under forced condition (a force constant of 50 kcal/mol), allowing motion of residues in the vicinity of the chromophore, realized the conversion to an all-trans C12–C13 *s*-trans conformation. Taking account of the photoconvertibility among Lumi, Batho, rhodopsin, and isorhodopsin, the cyclohexenyl moiety was kept in the same pocket as that of Batho and rhodopsin during the simulation. The resulting structure of opsin appreciably deformed the helical structure around Gly121 on TM3 (rmsd value of 0.74 for the backbone atoms). However, the backbone structures of the other helices remained almost unchanged (rmsd values of 0.02, 0.05, 0.02, 0.11, 0.04, and 0.26 for the backbone atoms in TM1, TM2, TM4, TM5, TM6, and TM7, respectively). The chromophore took a nearly planar conformation (-175 to 174° for C11–C12–C13–C14 and -173 to -179° for C9–C10–C11–C12) in the C9–C14 region and had a twisted C8–C9 bond (-155 to -161° for C7–C8–C9–C10). The PSB proton was turned over toward the Glu113 carboxylate, which was situated within a weak hydrogen bond distance of 3.1–3.8 Å.

A somewhat long time scale ($\sim 1 \mu\text{s}$) for conversion from Lumi to Meta I would be sufficient for a considerable alteration of the conformations of the chromophore and side chains surrounding the chromophore. Conformation of the entire chromophore and residues in the vicinity of the chromophore was explored for the Meta I structure by restrained molecular dynamics at 298 K for 300 ps. In the low-energy conformations generated by molecular dynamics simulation, the cyclohexenyl moiety was located at the interface between the extracellular loop(s) and the transmembrane region. This suggests that the extracellular loops have a role in controlling the conformational change of the chromophore in the Lumi to Meta I transition. The generated chromophore structures showed a nearly flat

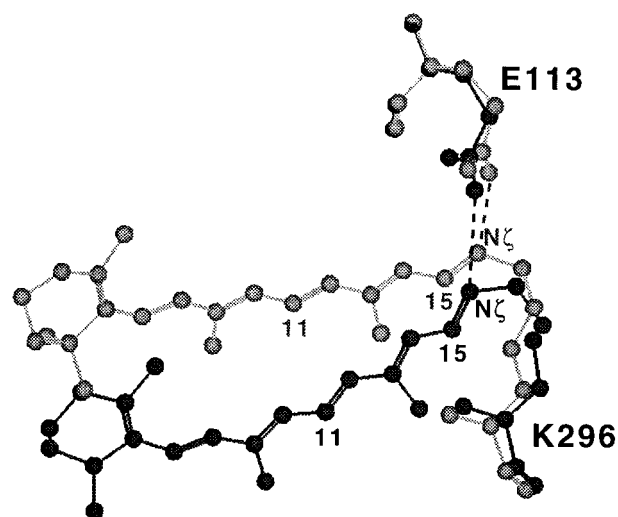


Figure 6. Lateral view of the chromophore in Lumi (black) and Meta I (gray). Only Glu113 and Lys296 of opsin are shown for clarity.

conformation in the acyclic portion ($180 \pm 2^\circ$ for the single bonds in 50 conformations). The flat conformation at the C11–C13 portion is consistent with the result obtained from solid-state NMR measurements.

The most stable structure showed various conformational changes in the chromophore and in the neighboring opsin residues. The geminal dimethyl group of the cyclohexenyl moiety lay on the Phe211 residue on TM5. The Phe207 residue on TM5 became proximal to the cyclohexenyl moiety (~ 4 Å). The Phe115 residue on TM3 was also close to the C5 methyl group (~ 4 Å). Thus, these three aromatic residues formed a new pocket for the cyclohexenyl moiety. The Thr118 residue made van der Waals contacts with the C9–C11 portion, sandwiching the C9–C10 double bond with the Tyr268 residue. The C9-methyl group was located 4.9 Å away from C α of Gly121, and far from the Phe261 residue (>10 Å). The C13-methyl group pointing toward the Gly121 and Trp265 residues was about 4 Å apart. The PSB nitrogen moved closer to the Glu113 carboxylate oxygen (2.8 Å), and thus the carboxylate was located at an appropriate position to receive a proton from the PSB. In Figure 6 the opsin-bound chromophore structures of Lumi and Meta I are superimposed. Upon neutralization of the PSB and the carboxylate, this intermediate could be converted to Meta II, the active form for signal transduction.³

Calculated UV Absorption Maxima for the Chromophore Structures. The photointermediates are well characterized by their UV absorption maxima. Hence, absorption maxima (λ_{max}) of the chromophore structures modeled in this study were estimated by the semiempirical quantum chemical program ZINDO.⁴⁸ The result of the calculation for each conformation of the photoactivated rhodopsins together with the dihedral angles for C9–C10–C11–C12 (α), C10–C11–C12–C13 (β), and C11–C12–C13–C14 (γ) is shown in Table 1.

The calculated values of the model structures were in good agreement with the observed values. The 5.4 Å charge separation between the PSB and the carboxylate appears to contribute to the red shift in rhodopsin. Blue shifts from Batho to Lumi and then to Meta I (Table 1) were consistent with the observed values for Lumi and Meta I implying that the change in the distances between the charged groups (3.3 and 2.8 Å, respectively) is the major factor contributing to the blue shifts. Conformations having modified-dihedral angles for β (rotamers

(48) Ridley, J.; Zerner, M. *Theor. Chim. Acta* **1973**, *32*, 111.

Table 1. Estimated Absorption Maxima of the Photoactivated Rhodopsin Chromophores

	α^a	β^b	γ^c	$\lambda_{\max}^{\text{(calc)}} \text{ (nm)}$	$\lambda_{\max}^{\text{(obs)}} \text{ (nm)}$
rhodopsin	167°	-4°	173°	495	498
Batho	-170°	-149°	-45°	528	540
Batho (rotamer 1)	-170°	-140°	-45°	543	
Batho (rotamer 2)	-170°	-170°	-45°	516	
Lumi	178°	177°	-176°	502	497
Meta I	-176°	-174°	-174°	492	478

^a C9–C10–C11–C12. ^b C10–C11–C12–C13. ^c C11–C12–C13–C14.

1 and 2) indicated that the twist of the C11–C12 double bond provides a large red shift up to ~ 30 nm (Table 1). Taking into account that the bathochromic shift takes place in the *s-cis* conformation of 1,3-diene,⁴⁹ the large bathochromic shift could be attributed to the C12–C13 *s-cis* conformation and the twisted C11–C12 double bond. It is intriguing that the twist of the double bond and the distance between the PSB and the carboxylate can be precisely controlled in the opsin structure but not in solution.

Discussion

To transfer the proton to the carboxylate at the Meta II stage, the PSB proton should orient toward the Glu113 carboxylate (that is, toward the extracellular site) *after* the photoisomerization reaction. Since the PSB portion is thought to turn over during the photoisomerization step,¹⁸ the PSB proton in rhodopsin is expected to point away from the Glu113 site. However, recent rhodopsin models have the chromophore PSB proton oriented toward the extracellular site from the very beginning.^{27,28} Therefore, the model described here is distinct from these previously reported rhodopsin structures and will not be compared with them.

The carboxylate group of Glu113 was located further away from the position expected from solid-state ¹³C NMR measurements.³⁹ Although an alternative reason for the large upfield shift of C12 is unclear, the presence of the Ala295 backbone carbonyl oxygen close to C12 (3.5 Å) could also account for the observed shift. The bathochromic shift of rhodopsin would then be attributed to the large 5.4 Å separation of the charged groups, as well as the rigidified chromophore bound to opsin.

The positive CD signal at 500 nm for rhodopsin has been correlated to a positive dihedral angle at the C12–C13 bond of the 11-*cis*-retinylidene chromophore from theoretical calculations.⁵⁰ Intriguingly, the model of the rhodopsin chromophore agrees well with this theoretical result. That is, the chromophore had a right-handed helical structure of three double bonds in the C9–C13 portion due to the positive dihedral angles for C9–C10–C11–C12 and C11–C12–C13–C14 as schematically depicted in Figure 7 (top). On the other hand, Batho shows a negative CD signal at 540 nm. In accord with this change of signal, the Batho chromophore had all negative dihedral angles for C9–C10–C11–C12, C10–C11–C12–C13, and C11–C12–C13–C14. The three double bonds, C9–C10, C11–C12, and C13–C14, thus formed a left-handed helical structure as depicted in Figure 7 (bottom). The twisted C11–C12 double bond reinforces the left-handed helical structure of the three double bonds. This structure may relate to the negative CD signal at 540 nm for Batho.

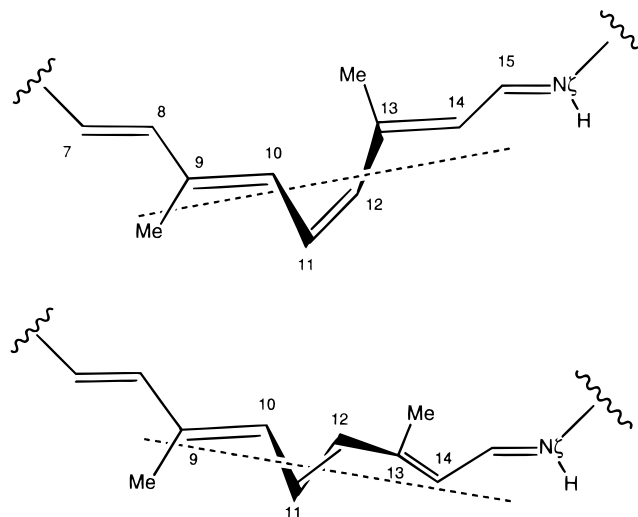


Figure 7. Helical conformations of the C9–C14 portions of the chromophore of rhodopsin (top) and Batho (bottom). The dihedral angles for C8–C9–C10–C11 and C11–C12–C13–C14 in the rhodopsin chromophore show positive values whereas the plane consisting of the C7–C8 and C9–C10 double bonds is located at the left-hand side of the plane consisting of the C13–C14 and C15–N ζ double bonds forming a negative dihedral angle. The C11–C12 bond of Batho denotes the twisted C11–C12 double bond. The dotted line indicates the axis of the helical structure.

The hydrogen bond network mediated by water molecules in the cavity appears to be important for G protein-coupled receptors (GPCR) belonging to the rhodopsin family, since the model suggested that the highly conserved Asp83 and Asn302 residues (Figure 1) are involved in this hydrogen bond network. In the photoconversion of the chromophore in rhodopsin, the motion of the surrounding water molecules could muffle the structural effect of the extremely rapid conformational change of the chromophore on opsin. The PSB proton oriented toward the interior of the protein in this rhodopsin model could achieve the reported fast deuterium exchange⁴⁰ through the putative structural water network connecting the PSB proton to the water molecule hydrogen bonded to the Glu113 carboxylate.

The twisted C12–C13 *s-cis* conformation of the Batho chromophore indicated simultaneous rotation of the C12–C13 bond during *cis*–*trans* isomerization of the C11–C12 bond. Liu and his colleagues discussed that simultaneous rotation of a double bond and a single bond is an allowed process in a photoexcited state and proposed a simultaneous rotation of the C10–C11 bond in the photoconversion (concerted-twist model).²⁵ However, the successful conversion of a C10–C11 bond-locked analogue to a Batho structure^{26,51} led to the alternative model of the simultaneous C12–C13 bond rotation.²⁶ Recently, the concerted-twist isomerization was experimentally and computationally demonstrated in the photoisomerization of previtamin D.⁵² Thus, it is likely that the concerted-twist (hula-twist) is a general process in the photochemistry of polyenes.

The 9-*cis*-retinylidene chromophore **2** in isorhodopsin is also converted to the same Batho structure by photoirradiation.⁵ This conversion could be achieved by the simultaneous C12–C13 bond rotation with the *cis*–*trans* isomerization of the C9–C10 double bond. This two-bond rotation should require a larger conformational space, which accounts for a longer isomerization

(51) Sheves, M.; Albeck, A.; Ottolenghi, M.; Bovee-Geurts, P. H. M.; De Grip, W. J.; Einterz, C. M.; Lewis, J. M.; Schaechter, L. E.; Kliger, D. S. *J. Am. Chem. Soc.* **1986**, *108*, 6440.

(52) Müller, A. M.; Lochbrunner, S.; Schmid, W. E.; Fuss, W. *Angew. Chem., Int. Ed.* **1998**, *37*, 505.

(49) Allinger, N. L.; Miller, M. A. *J. Am. Chem. Soc.* **1964**, *86*, 2811.
(50) Buss, V.; Kolster, K.; Terstegen, F.; Vahrenhorst, R. *Angew. Chem., Int. Ed.* **1998**, *37*, 1893.

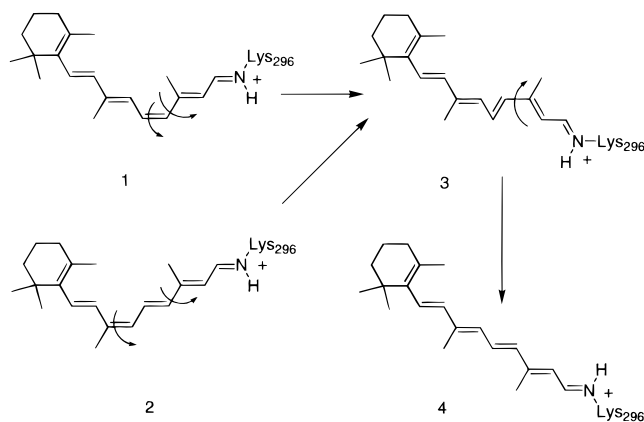


Figure 8. Proposed scheme for photoisomerization of 11-*cis* and 9-*cis* chromophores (**1** and **2**) to the 12-*s-cis* all-trans chromophore (**3**) and the 12-*s-trans* all-trans chromophore (**4**).

time (~ 600 fs) for the 9-*cis*-chromophore than that (200 fs) for the 11-*cis*-chromophore.⁵³ Thus, the photochemical interconversion among rhodopsin, isorhodopsin, and Batho may commonly be accompanied by a simultaneous rotation of the C12–C13 bond (Figure 8).

The C12–C13 *s-cis* conformation should contribute to the red shift of the absorption maximum of the Batho chromophore. The ZINDO estimation of the absorption maximum demonstrated that an approximately 30° twist at the C11–C12 double bond should bring about a large red shift. It is thus conceivable that the strained structure of the Batho chromophore stems from the twist of the C11–C12 double bond. The release of strain energy of the twisted double bond would lead to further conformational change of the chromophore, affecting the opsin structure.

The steric interactions between the C13-methyl group and opsin during the *s-cis* to *s-trans* conversion would account for the thermal instability of the C13-demethylated chromophore in Batho,⁵⁴ and would be the first process in the energy transfer from the photoexcited chromophore to opsin. The absorption maximum calculated for the resulting C12–C13 *s-trans* all-trans chromophore is consistent with that observed for the Lumi chromophore (Table 1).

Restoration of a relaxed helical structure of TM3 from the deformed helix generated in the Batho to Lumi transition may cause rearrangement of the surrounding transmembrane helices. Although a substantial movement of the transmembrane helices would occur mainly at the cytoplasmic site, it would affect the conformation of the chromophore. Therefore, the calculated absorption maximum for the chromophore in the Meta I model is at best accurate within the limit of the conditions used in the simulation. The putative Meta I structure indicated that the cyclohexenyl moiety was accommodated in a different binding pocket. A photoaffinity-labeling experiment using 11-*cis*-retinal analogue substituted with the *o*-dimethyl *p*-trifluoromethyl-diazirine phenyl group for the cyclohexenyl moiety resulted in labeling a wide range of residues on TM3 and 6,⁵⁵ indicating the presence of multiple binding sites for the chromophore. This experimental result would support the existence of a distinct

binding site for the cyclohexenyl moiety of the Meta I chromophore. The conformational change of the chromophore also brought the PSB nitrogen closer (2.8 Å) to the carboxylate oxygen. This short distance should facilitate the proton transfer from the PSB to the carboxylate and trigger the conversion from Meta I to Meta II. This conversion would then accompany rigid-body motions of the transmembrane helices in a period (ca. milliseconds) longer than the previous processes (Batho through Meta I). This motion of the transmembrane helices complicates the model building of the structure for Meta II.

Conclusion

The present study is an attempt to delineate the mechanism of primary photoactivation of rhodopsin through modeling of the photointermediates by the use of a three-dimensional α -structure model of the transmembrane helices of opsin and by means of restrained molecular dynamics by enforcing an isomerization. The results described above indicate that the transmembrane model of rhodopsin appears to be useful for understanding the photoisomerization and the photoactivated conformations of the chromophore. However, as for most calculations, it is not appropriate to discuss the results in a quantitative manner.

The opsin shift in the rhodopsin chromophore could be mainly attributed to the distance between the PSB and the counterion as well as the conformation rigidly held in opsin. The red shift in the Batho chromophore could be attributed to the twist of the C11–C12 double bond and the C12–C13 *s-cis* conformation. The photoconversion is expected to proceed through simultaneous rotation of the C12–C13 bond, leading to a twisted C12–C13 *s-cis* all-trans chromophore for Batho. This conformation correlated well to resonance Raman and CD spectra. In particular, the helical structures formed by the C9–C10, C11–C12, and C13–C14 double bonds were consistent with the CD signals of rhodopsin and Batho. Conformational change of the Batho chromophore to Lumi would cause deformation of TM3 by steric interaction between the 13-Me group and opsin during rotation of the C12–C13 bond. A further conformational change of Lumi to Meta I accompanied large conformational changes of the chromophore and the residues in the vicinity of the chromophore. The PSB proton moved to an appropriate position for proton transfer to the carboxylate of Glu113, which triggers the conversion from Meta I to Meta II, the active form of rhodopsin.

Acknowledgment. The author would like to thank Dr. J. M. Baldwin of MRC Laboratory, UK for her generous gift of the α coordinates of rhodopsin structure model and is grateful to Dr. S. Imajo of Suntory Institute for Biomedical Research, Dr. K. Yoshihara of Suntory Institute for Bioorganic Research and Professor Y. Shichida of Kyoto University for their generous discussion. Dr. Y. Kato-Toma is also gratefully acknowledged for critically reading the manuscript. A part of this work has been supported by CREST of JST (Japan Science and Technology).

Supporting Information Available: Cartesian coordinates for the photoactivated intermediates (PDF). This material is available free of charge via the Internet at <http://pubs.acs.org>.

(53) Schoenlein, R. W.; Peteanu, L. A.; Wang, Q.; Mathies, R. A.; Shank, C. V. *J. Phys. Chem.* **1993**, *97*, 12087.

(54) Shichida, Y.; Kropf, A.; Yoshizawa, T. *Biochemistry* **1981**, *20*, 1962.

(55) Nakayama, T. A.; Khorana, H. G. *J. Biol. Chem.* **1990**, *265*, 15762.